Axial Flow Damping Test of the Full Scale US-APWR Fuel Assembly

Non-Proprietary Version

August 2013

© 2013 Mitsubishi Heavy Industries, Ltd.

All Rights Reserved

<u>Abstract</u>

The US-APWR plant is designed to withstand seismic/LOCA loading as part of safety analysis. Structural damping of fuel assembly in reactor coolant plays an important role to accurately characterize seismic/LOCA fuel assembly response in the analysis. The damping ratios of the fuel assembly vary depending on the coolant operating conditions (e.g., still water, flowing water). In the past, damping response evaluations under axial flow conditions have been conducted and the results were published by several facilities.

This report addresses the axial flow damping (AFD) response for a representative US-APWR mock-up fuel assembly under still water and axial flow conditions, with variable displacements, coolant flow rates, and temperature conditions. This testing is based on the past MHI experience with conventional 12-ft fuel assembly vibration characteristic testing under axial flow conditions.

Tests were performed at room temperature in the still water testing, and at three different temperature conditions with axial flow. Various flow rates, dependent on the thermal design flow (TDF), were tested at each temperature. Multiple fuel assembly initial displacements were applied at each condition. Based on the test, the amplitude dependent damping ratio and frequency values were obtained.

The AFD test results show that:

These results will be used to determine input to the US-APWR fuel seismic response analysis to account for the AFD effect (Reference 1) and the results will be shown in the next revision of MUAP-08007 "Evaluation Results of US-APWR Fuel System Structural Response to Seismic and LOCA loads" (Reference 2).

Table of Contents

List of Tables

List of Figures

1.0 INTRODUCTION

This report documents the test setup, procedures, conditions, and results of the pluck test under still and axial flow conditions (hereafter, axial flow damping (AFD) test), performed on a mock-up fuel assembly. This testing was performed to appropriately account for the AFD effect in the US-APWR fuel seismic response analysis.

All tests were conducted in compliance with ASME NQA-1 "Quality Assurance Program Requirements for Nuclear Facilities" (Reference 3).

2.0 GENERAL DESCRIPTION

2.1. Test Facility

The mock-up fuel assembly is installed in a closed loop, isothermal fuel assembly hydraulic test facility. The test loop consists primarily of two circulation pumps, a test section, a water storage tank, a pressure control tank and a heat exchanger. The internals of the flow housing surrounding the mock-up fuel assembly insertion area is comprised of a rectangular enclosure that is used to direct flow into the full scale mock-up fuel assembly in a controlled manner. The AFD test was conducted using the test facility shown in Figure 2.1-1.

The hydraulic test facility, located at the Nuclear Development Corporation (NDC), is used to perform the AFD testing, as well as investigate long term fuel rod fretting wear, hydraulic fuel rod vibration properties, pressure loss, and lift force measurements of the fuel assembly.

2.2. Fuel Assembly

The design specification and the schematic overview for the US-APWR test fuel assembly are shown in Table 2.2-1 and Figure 2.2-1, respectively.

The tests are performed on a mock-up fuel assembly that is hydraulically and mechanically the same as the US-APWR 14-ft fuel assembly. The test assembly consists of an Inconel-718 top and bottom grid spacers, nine Zircaloy-4 intermediate grid spacers, 264 fuel rods, 24 control rod guide thimbles and one instrumentation tube. The fuel rods are filled with lead-antimony pellets to simulate the standard fuel rod weight. The rods contain a preloaded coil spring in the upper plenum and a spacer in the lower plenum. Spring forces of the intermediate grid spacers are set to simulate end of life (EOL) condition. Fuel assembly damping is determined by the effect of both structural damping and AFD. Hydraulic drag forces, which are dominant for the AFD effect, are theoretically determined by the fluid properties such as density and viscosity, flow velocity and the geometric properties of the fuel assembly that are not affected by irradiation. The BOL fuel assembly has much higher stiffness than the EOL fuel assembly and is consequently not the limiting case in the seismic response evaluation. Therefore, the fuel assembly simulating EOL condition with relaxed spring force is applied to the AFD test.

Table 2.2-1   Test Fuel Assembly Design Specifications

Fuel Assemblies	
Fuel Rod Array	17 x 17
Overall Fuel Rod Length	14 ft (181.5 in / 4610mm)
Number of Fuel Rods	264
Number of Control Rod Guide Thimbles	24
Number of In-Core Instrumentation Guide Tube	1
Number of Grid Spacers	11
Fuel Rods	
Outer Diameter	0.374 in (9.50mm)
Cladding Thickness	0.0224 in (0.570mm)
Active Fuel Length	165.4 in (4,200mm)
Pellet Material	Antimony -Lead
Pellet Diameter	0.322 in (8.19 mm)
Pellet Density	simulating UO_2 weight
Plenum	Upper & Lower
Materials	
Cladding	ZIRLO^{TM}
Top & Bottom Grid Spacers	Inconel 718
Intermediate Grid Spacers	Zircaloy-4 (simulating EOL spring force)
Control Rod Guide Thimbles and In-Core Instrumentation Guide Tube	Zircaloy-4
Nozzles	Stainless Steel
Holddown Springs	Inconel 718*

Note) * Inconel 718 is a nickel-chromium-iron alloy 718

Heat Exchanger

Pressure Control Tank

Water Storage Tank

Bypass Line

Pump

Pump

Test Section
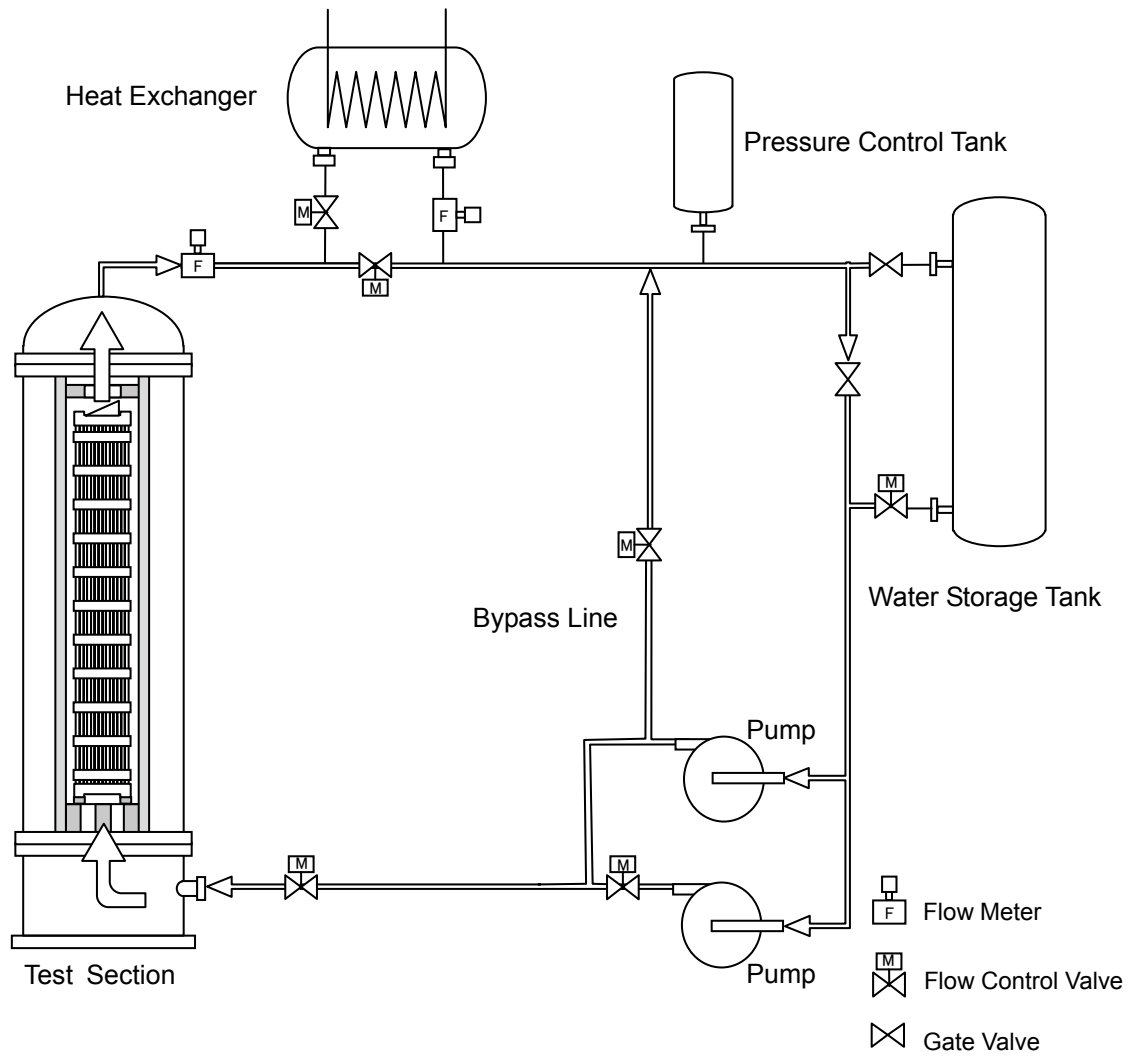
Flow Meter

Flow Control Valve

Gate Valve

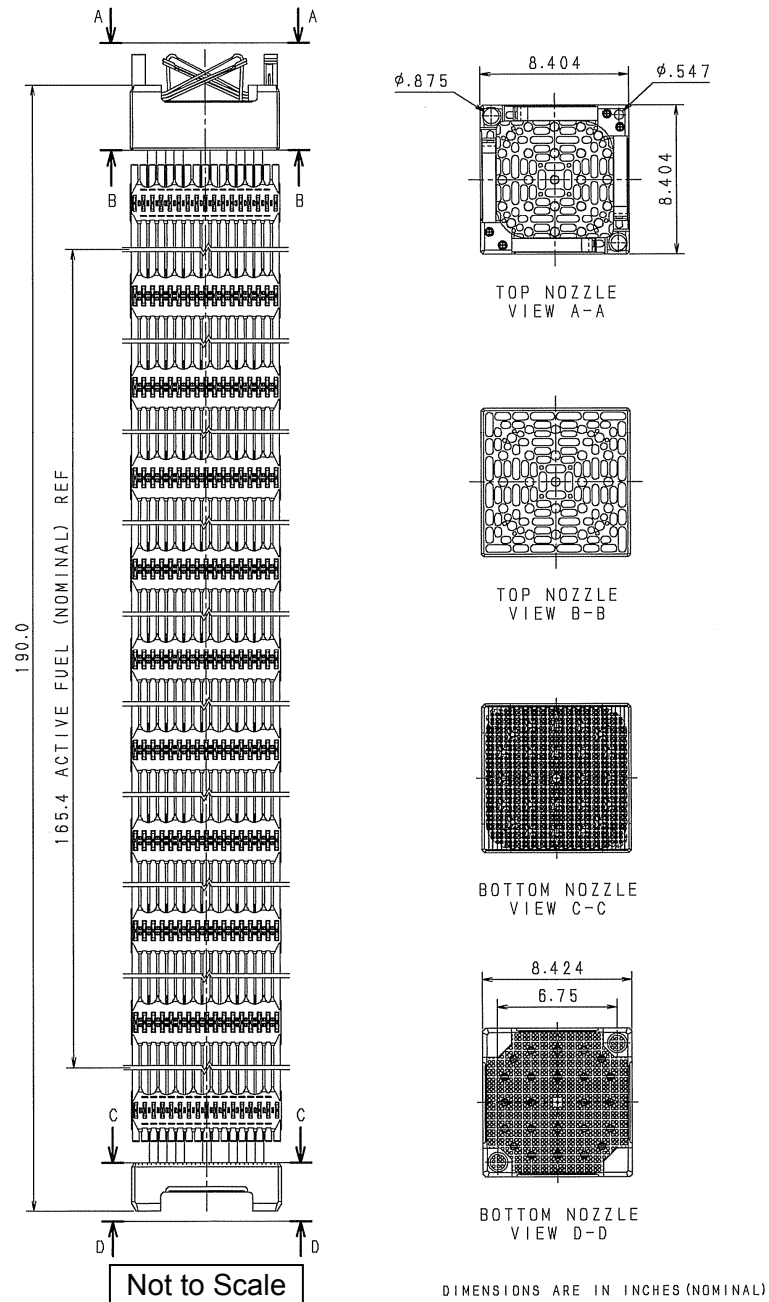**Figure 2.1-1   Fuel Assembly Hydraulic Test Facility**

Figure 2.2-1   Schematic View of US-APWR Fuel Assembly

3.0 TEST PROCEDURE

3.1. Lift Force Measurement

The objective of the lift force measurement test is to evaluate water flow rates through the mock-up fuel assembly. To achieve objective, the correlation between effective rod bundle flow velocity and pump flow rate is determined by measuring the lift force for the fuel assembly at different flow conditions for each temperature condition; where the rod bundle flow velocity is the flow rate in the fuel rod bundle. Since the AFD test section has a gap between the fuel assembly and the test section walls, the rod bundle flow velocity cannot be directly determined from the pump flow rate.

The fuel assembly lift force test used the same test equipment and setup as the AFD test. In order to measure the fuel assembly lift force, four load cell transducers are installed on the locations where the fuel assembly is in contact with the lower core plate to transmit lift force data.

The lift force measurement test was performed in advance of the AFD test. An overview of the test procedure is shown in Figure 3.1-1.

The lift force test was performed for each condition seen in Table 3.1-1.

First, the water temperature in the test loop was set to the desired temperature, and the measurement systems were confirmed to be properly working. Then, the buoyancy (background) lift force measurement was taken in the still water condition. Next, measurements were taken, starting at a flow rate of [   ], until the measured lift force exceeded the estimated 100%TDF lift force. Finally, the flow rate was reduced to the still water condition. These steps were performed at each temperature condition.

Using the data from the testing, the effective rod bundle flow velocity is evaluated using the determined buoyancy force, the determined lift force, and the fuel assembly pressure coefficient data in Reference 4. The results give the relationship between the test loop flow and the effective rod bundle flow velocity in the mock-up fuel assembly.

3.2. Axial Flow Damping Tests

The objective of the AFD test is to determine the vibration characteristics, such as damping ratio and frequency, of the mock-up fuel assembly when axial flow conditions are introduced. The data will be used to determine damping ratio and frequency input into the FINDS analyses (Reference 1). Damping ratios will be assessed and adjusted taking into account the differences between the test conditions and the reactor operating condition, if necessary.

A test fuel assembly was loaded into the test section of the hydraulic test loop shown in Figure 2.1-1. The top and bottom nozzles are aligned by fuel-guide pins on corresponding upper and lower core plate simulators, and the top nozzle hold-down springs are compressed.

To measure the fuel assembly frequency and damping characteristics, linear variable differential transformers (LVDTs) are used to track the fuel assembly displacement versus time and are positioned at the middle grid spacer to measure maximum fuel assembly displacement. Their locations can be seen in Figure 3.2-1. The initial displacement of the mock-up fuel

assembly is generated with [   ] equipment.

An overview of the test procedure is shown in Figure 3.2-2. The AFD testing is run for each temperature test condition seen in Table 3.2-1. First, the water temperature is set in the test loop to the desired temperature, and the measurement systems are confirmed to be properly working. The [   ] equipment is checked and background measurements of LVDTs are taken in the still water condition. Then, the pump flow rate is set and measured. The initial displacement is added to the fuel assembly by the [   ] equipment under constant flow conditions and released. Finally, the fuel assembly is released and the displacement time history of the middle grid is measured. These measurements are taken for each initial displacement condition shown in Table 3.2-1. After each initial displacement condition is run for a given temperature setting, the flow rate is changed.   After the tests under all the combinations of initial displacements and flow rates are performed, the temperature condition is changed until all tests are complete. Each test condition is repeated three times, to ensure repeatability.

In addition, pluck tests are conducted to study the frequency and damping characteristics under still water condition and axial flow conditions.

3.3.   AFD Test Conditions

The test matrix is shown in Table 3.2-1. The test parameters are initial displacement of the fuel assembly, temperature, and flow rate.

The gaps between the mock-up fuel assembly and the wall of the test section are shown in Table 3.3-1. A [   ] is set as the maximum initial displacement distance. In the orthogonal direction, a [   ] is set to avoid contact between the mock-up fuel assembly and the test wall during vibration.

3.3.1.   Initial Displacement Conditions

The initial displacement parameter evaluates the damping and frequency dependencies on amplitude. Testing took place at the test section with initial displacements of [   ], as shown in Table 3.2-1. These four initial displacement points can be used to interpolate the amplitude impact on frequency and damping of the fuel assembly.

3.3.2.   Temperature Conditions

Testing is performed at [   ], as shown in Table 3.2-1.

Both water density and kinematic viscosity are dependent on water temperature and therefore affect the vibration response. However, the MHI conventional 12-ft fuel assembly testing with axial flow conditions showed that the temperature effect of AFD appears to be very small up to the reactor operating condition from the maximum test temperature (Reference 5). Therefore, MHI expects that the additional testing will confirm the temperature dependency of the AFD effect on the US-APWR fuel assembly. Damping ratios are interpolated from the test condition to reactor operating condition, if necessary.

3.3.3. Flow Rate Conditions

The flow rate conditions to evaluate the flow rate dependency of the AFD effect are shown in Table 3.2-1. The effective flow rate inside the fuel rod bundle is evaluated using the fuel assembly lift force measurement test, as described in Section 3.1, and the pressure drop coefficient. The appropriateness of these methods is demonstrated in Reference 3.

The flow rate conditions are based on the TDF rate in the US-APWR reactor. In order to study the flow rate dependency of frequency and damping under axial flow conditions, [   ] conditions are used as the test parameters. This variation is aimed at obtaining sufficient data to adequately simulate the AFD effect for reduced reactor coolant flow conditions in the fuel seismic response analysis.

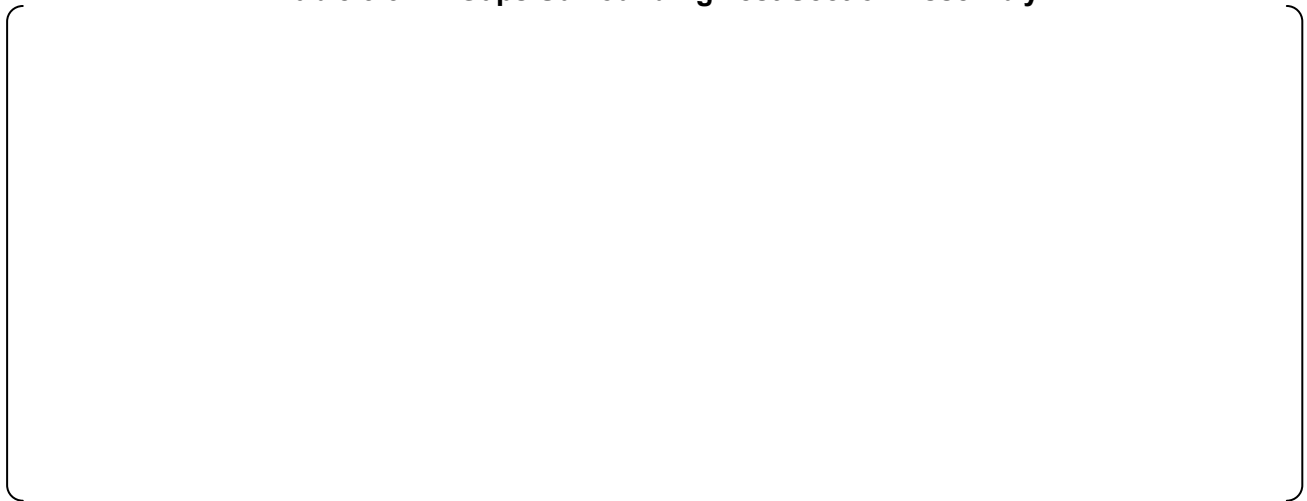**Table 3.1-1   Test Matrix for Lift Force Measurement Test**

Table 3.2-1   Test Matrix for Axial Flow Damping Test

Table 3.3-1   Gaps Surrounding Test Section Assembly

```
            ┌──────────────────────────────┐
            │ 1. Set Water Temperature      │
            └──────────────────────────────┘
                          │
                          ▼
            ┌──────────────────────────────┐
            │ 2. Check Measurement Systems  │
            └──────────────────────────────┘
                          │
                          ▼
            ┌──────────────────────────────┐
            │ 3. Background Measurement     │
            └──────────────────────────────┘
                          │
                          ▼
            ┌──────────────────────────────┐
            │ 4. Lift Force Measurement     │◄──┐
            └──────────────────────────────┘   │
                          │                     │
                          ▼                     │
                    ╱─────────────╲             │
                   ╱ 5. Lift Force ╲      No    │
                  ╱  Measurement    ╲───────────┘
                   ╲ above 100%TDF  ╱
                    ╲─────────────╱
                          │
                          ▼
            ┌──────────────────────────────┐
            │ 6. Background measurement     │
            └──────────────────────────────┘
```

Increase Water Temperature

Increase Water Flow
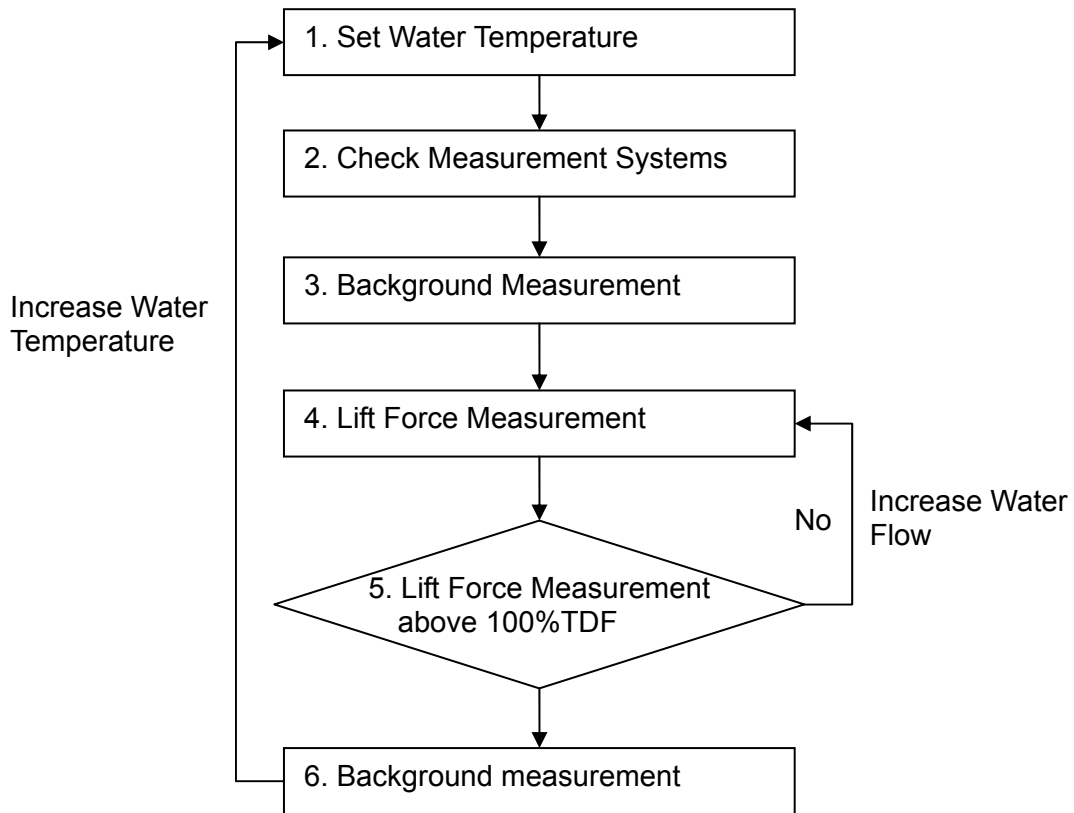
Figure 3.1-1   Overview of Lift Force Measurement Test Procedure
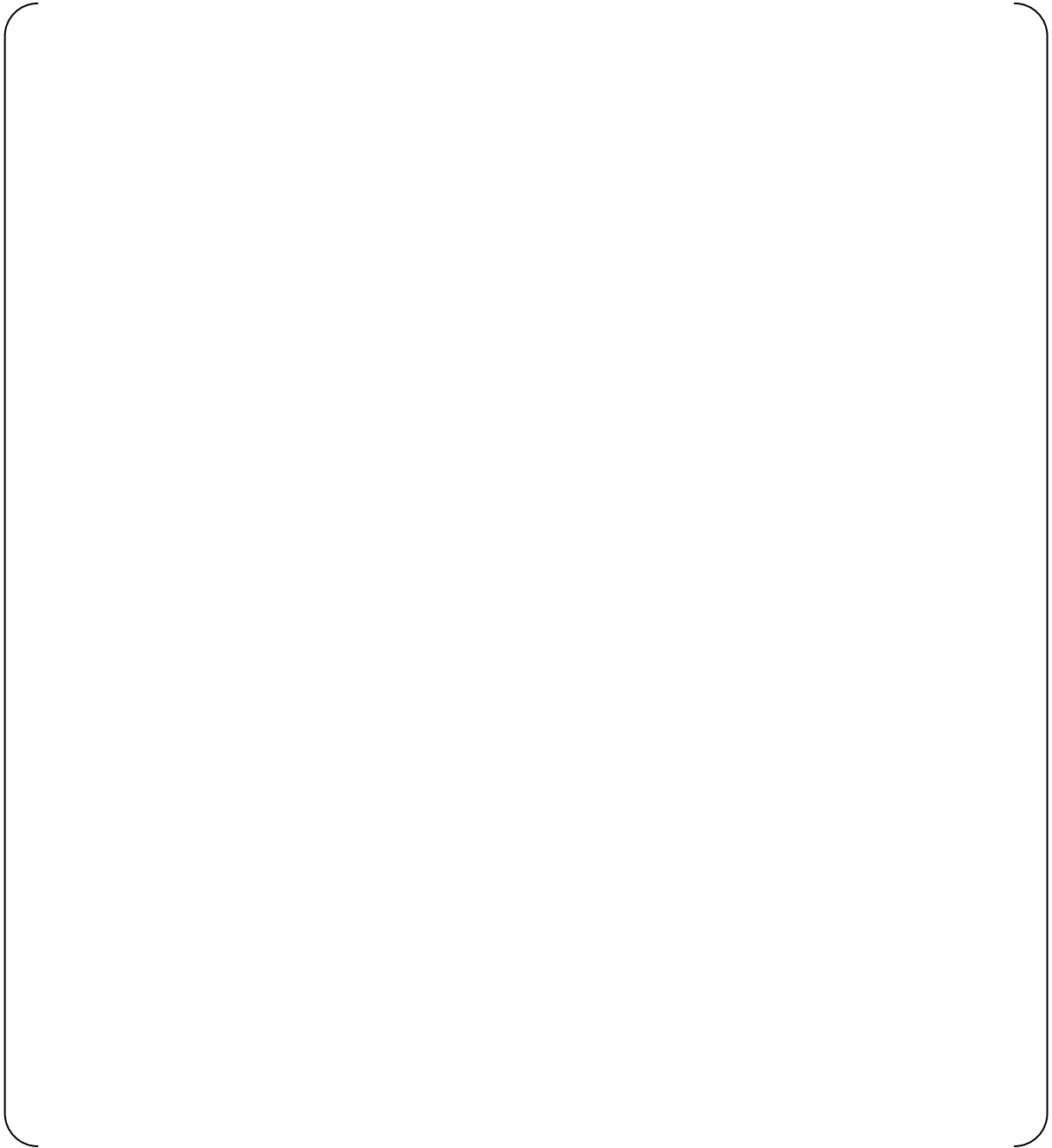
Figure 3.2-1   Schematic View of Test Section

```
┌─────────────────────────────────┐
│  1. Fill Test Loop with Water    │
└─────────────────────────────────┘
                 │
                 ▼
┌─────────────────────────────────┐
│  2. Set Water Temperature        │
└─────────────────────────────────┘
                 │
                 ▼
┌─────────────────────────────────┐
│  3. Check Measurement Systems    │
└─────────────────────────────────┘
                 │
                 ▼
┌───────────────────────────────────────┐
│  4. Check [              ] Equipment   │
└───────────────────────────────────────┘
                 │
                 ▼
┌─────────────────────────────────┐
│  5. LVDTs Background Measurement │
└─────────────────────────────────┘
                 │
                 ▼
┌─────────────────────────────────┐
│  6. Set Pump Flow Rate           │
└─────────────────────────────────┘
                 │
                 ▼
┌─────────────────────────────────┐
│  7. Add Initial Displacement     │
└─────────────────────────────────┘
                 │
                 ▼
┌───────────────────────────────────────┐
│  8. Release [             ] Equipment  │
└───────────────────────────────────────┘
                 │
                 ▼
┌─────────────────────────────────┐
│  9. Measure Vibration Response   │
└─────────────────────────────────┘
                 │
                 ▼
         ╱ 10. Initial Displacement ╲  ── No
         ╲ Conditions Complete?     ╱
                 │ Yes
                 ▼
         ╱ 11. Pump Flow Rate ╲
         ╲ Conditions Complete? ╱
```
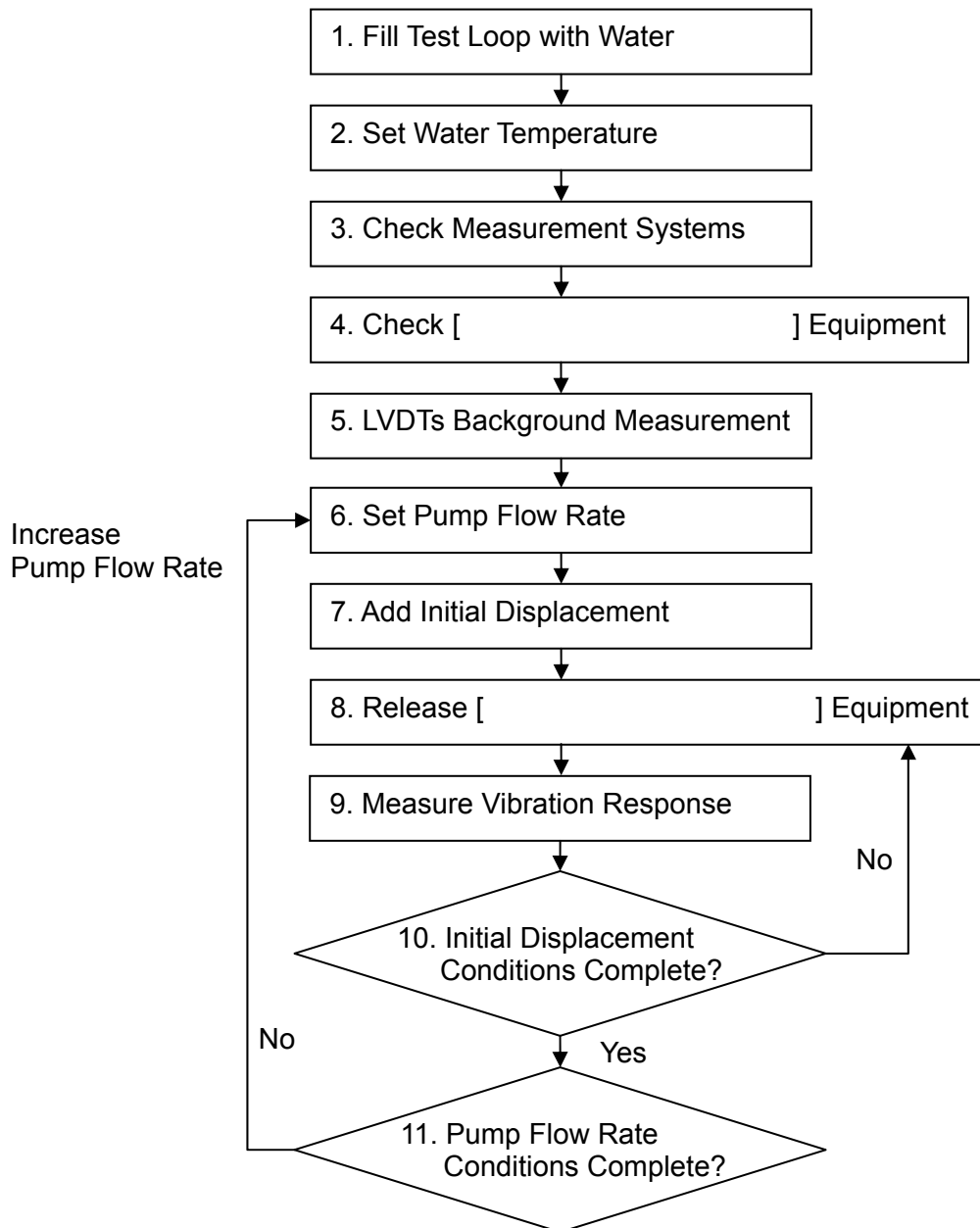
Increase
Pump Flow Rate

No

No

Yes

Figure 3.2-2   Overview of AFD Test Procedure for Each Temperature

4.0 DATA REDUCTION METHOD

4.1. Lift Force Measurement Test

To evaluate water flow rates through the mock-up fuel assembly, the correlation between effective rod bundle flow velocity and pump flow rate is needed. This relationship is determined by measuring the lift force for the fuel assembly at different temperature and flow conditions and then using the measurements to estimate the effective rod bundle flow velocity. This correlation can be evaluated using the scheme presented in Figure 4.1-1. Table 3.1-1 shows the various test loop conditions used during the test. Table 4.1-1 shows the dimension values used in the data reduction calculations.

In the data reduction, a second order curve is first used to approximate the relationship between the measured fuel assembly lift force and measured pump flow rate. Coefficients a and b, in Equation 4.1-1, are solved to give a best fit relation between lift force and pumps flow rate.

$$F = a \times Q^2 + b \times Q \qquad \text{(Equation 4.1-1)}$$

Where,

F: Measured lift force of fuel assembly (kN)

Q: Pumps flow rate (m^3/h)

a, b: Coefficients

Next, the fuel assembly lift force is shown in Equation 4.1-2. This equation uses the fuel assembly pressure coefficient determined from Figure 4.1-2, which is based on prior US-APWR testing (Reference 3). The determined pressure drop coefficient is shown in Figure 4.1-2 and uses the Reynolds number. The related Reynolds number equation is listed in Equation 4.1-3.

$$F' = A \times \varsigma \times \frac{\rho v^2}{2} \qquad \text{(Equation 4.1-2)}$$

Where,
F': Lift force (N)
A: Rod bundle cross section (m^2)
ζ: Pressure drop coefficient
ρ: Water density (kg/m^3)
v: Rod bundle average flow velocity (m/s)

$$\mathrm{Re} = \frac{De}{\upsilon}v$$ (Equation 4.1-3)

Where,
Re： Reynolds Number (-)
De： Hydraulic Equivalent Diameter (m)
υ ： Viscosity (m^2/s)

By solving Equation 4.1-2, v can be obtained by the following equation.

$$v = \sqrt{\frac{2F^{'}}{A\rho\varsigma}}$$ (Equation 4.1-4)

The relation between the rod bundle average flow velocity v and the pump flow rate Q can be solved for. This can be done by substituting for the variables in the right hand side of Equation 4.1-4 using constants, Equations 4.1-3 and Figure 4.1-2, and the relation between lift force and pump flow rate solved for earlier. Additionally, the relation between the rod bundle average flow velocity and the lift force can be solved for.

The effective volumetric rod bundle flow velocity can be determined using Equation 4.1-4 and Equation 4.1-5.

$$Q^{'} = 3600 \times A \times v$$ (Equation 4.1-5)

Where,
Q'： Effective rod bundle flow velocity (m^3/h)
A： Effective flow area (m^2)
v： Rod bundle flow velocity (m/s)

4.2. Axial Flow Damping Test

The amplitude dependent damping ratios are obtained for the AFD tests using the decrement ratio between each successive peak of the fuel assembly oscillation (the half-cycle amplitude). This method models the response of an under-damped system, based on classical vibration theory. General solutions of the classical vibration theory and free vibration equation can be seen in Reference 6, the derivation of the methods used is shown via the following methods.

A generic free vibration equation with a mass, spring, and viscous damper system has the form shown below.

$$m\ddot{x} + c\dot{x} + kx = 0$$ (Equation 4.2-1)

Where,
  m : mass
  c : damping coefficient
  k : spring stiffness

The following equations show the expressions that are used for the un-damped natural frequency (ω_n), critical damping coefficient (c_c), and a defined non-dimensional damping ratio (ζ, hereafter, damping ratio), respectively.

$$\omega_n^2 = \frac{k}{m}$$ (Equation 4.2-2)

$$c_c = 2\sqrt{mk}$$ (Equation 4.2-3)

$$\zeta = \frac{c}{c_c}$$ (Equation 4.2-4)

Equations 4.2-2 through 4.2-4 can be combined with Equation 4.2-1, resulting in Equation 4.2-5.

$$\ddot{x} + \frac{c}{m}\dot{x} + \frac{k}{m}x = 0$$

$$\ddot{x} + \frac{c_c\zeta}{m}\dot{x} + \omega_n^2 x = 0$$

$$\ddot{x} + \frac{2\sqrt{mk}\zeta}{m}\dot{x} + \omega_n^2 x = 0$$

$$\ddot{x} + 2\omega_n\zeta\dot{x} + \omega_n^2 x = 0$$ (Equation 4.2-5)

Equation 4.2-5 can be solved as shown below.

$$x = Xe^{-\zeta\omega_n t}\cos(\sqrt{1-\zeta^2}\,\omega_n t + \phi)$$ (Equation 4.2-6)

X and ϕ are determined from the initial displacement and velocity condition.

The equation is shown below for the frequency with damping (ω_d), when the period of one cycle is set to be τ_d.

$$\omega_d = \frac{2\pi}{\tau_d} = \omega_n\sqrt{1-\zeta^2}$$ (Equation 4.2-7)

In the AFD tests, the decay under the axial flow condition is so rapid due to the hydraulic drag force that peaks after the first half cycle cannot be clearly observed. This can be seen in Figure 4.2-1, which shows a schematic figure of a fuel assembly's decay motion under axial flow. In these cases, dependent damping ratios are accurately calculated from the initial displacement and the first negative peak.

Also shown in Figure 4.2-1 are the initial displacement (x_0) and amplitude displacement at the first negative peak (x_1) of the response, respectively.

The time difference between the starting point of the free vibration and the first negative peak is defined as (Δt). This is calculated from Equation 4.2-7 and is shown in the equation below.

$$\Delta t = \frac{\tau_d}{2} = \frac{\pi}{\omega_n \sqrt{1-\zeta^2}}$$
(Equation 4.2-8)

For the free vibration equation case with initial displacement, ϕ can be set to be zero, Equation 4.2-6 can be rewritten as shown below.

$$x = x_0 e^{-\zeta \omega_n t} \cos(\sqrt{1-\zeta^2}\, \omega_n t)$$
(Equation 4.2-9)

Here, the amplitude displacement at the first negative peak (x_1) can be calculated by substituting Δt for t in Equation 4.2-9. It's important to note that x_0 and x_1 have opposite signs of each other.

$$
\begin{aligned}
x_1 &= x_0 e^{-\zeta \omega_n \Delta t} \cos(\sqrt{1-\zeta^2}\, \omega_n \Delta t) \\
&= x_0 e^{-\zeta \omega_n \cdot \frac{\pi}{\sqrt{1-\zeta^2}\,\omega_n}} \cos(\sqrt{1-\zeta^2}\,\omega_n \cdot \frac{\pi}{\sqrt{1-\zeta^2}\,\omega_n}) \\
&= x_0 e^{-\frac{\pi\zeta}{\sqrt{1-\zeta^2}}} \cos\pi \\
&= -x_0 e^{-\frac{\pi\zeta}{\sqrt{1-\zeta^2}}}
\end{aligned}
$$

Therefore,

$$-\frac{x_0}{x_1} = e^{\frac{\pi\zeta}{\sqrt{1-\zeta^2}}}$$
(Equation 4.2-10)

The logarithmic decrement (δ), obtained from the vibration test, is defined in Equation 4.2-11. It can be combined with Equation 4.2-10 to obtain Equation 4.2-12.

$$\delta = \ln\left(-\frac{x_1}{x_0}\right) \qquad \text{(Equation 4.2-11)}$$

$$\delta = \frac{\pi\zeta}{\sqrt{1-\zeta^2}} \qquad \text{(Equation 4.2-12)}$$

Equation 4.2-12 can be solved for ζ as shown below. Here the damping ratio ζ can be obtained from the displacement (δ) observed in the vibration test.

$$\zeta = \frac{\delta}{\sqrt{\pi^2 + \delta^2}} \qquad \text{(Equation 4.2-13)}$$

Additionally, frequency with damping can be obtained as shown below from the time difference between the free vibration starting point and the first negative peak.

$$f_d = \frac{1}{2\Delta t} \qquad \text{(Equation 4.2-14)}$$

The derived ζ and f_d obtained in the same manner can be obtained for a slow decay vibration such as a still water condition without axial flow. With slow decay vibration, however, more ζ and f_d data can be obtained from not only the first half cycle but also successive half cycles because of more visible peaks.

Table 4.1-1   Dimension Values Used for Lift Force Calculation

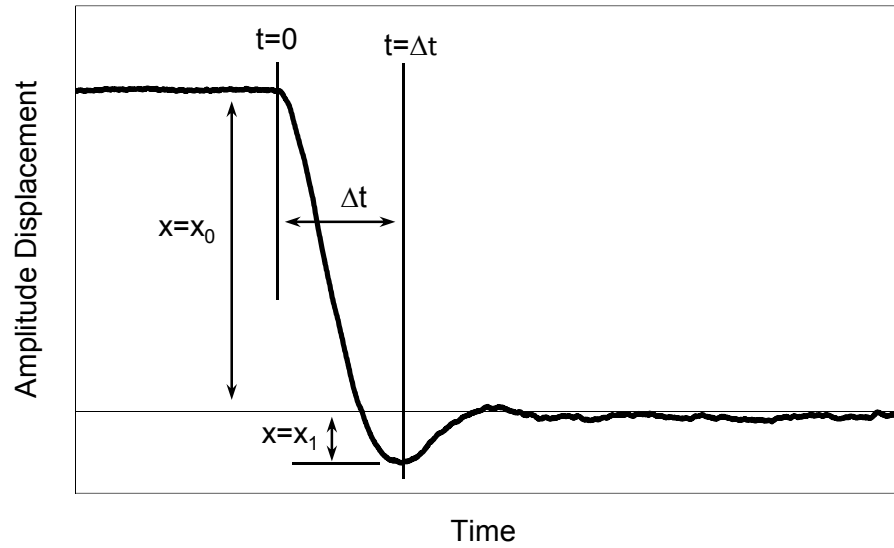| Dimension or Property	Value
Fuel Rod Diameter (mm)	9.5
Thimble Clad Diameter (mm)	12.24
Hydraulic Equivalent Diameter (mm)	[ ]
Rod Bundle Width (mm) *	[ ]

 * Value per a fuel assembly in the US-APWR core

Figure 4.1-1   Evaluation Scheme of Lift Force Measurement Test
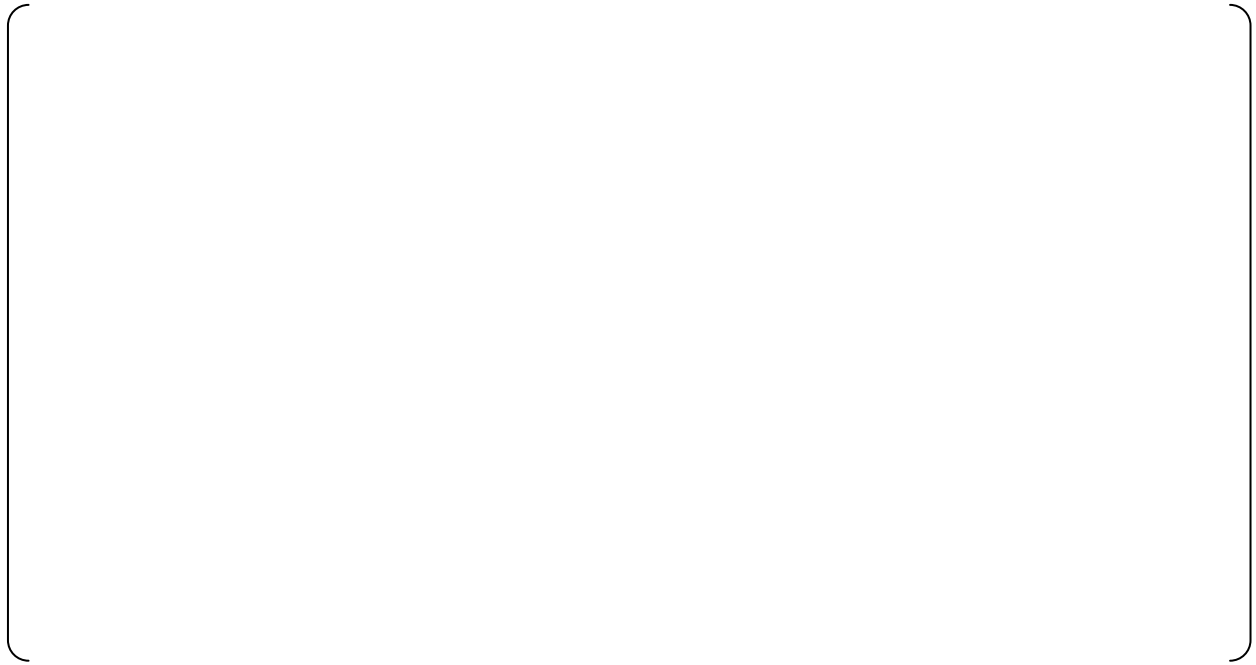
Figure 4.1-2   Fuel Assembly Pressure Loss Coefficient

Figure 4.2-1   Schematic of Fuel Assembly Decay Motion in Flowing Water for Mock-up Fuel Assembly

5.0 TEST RESULTS AND COMPARISON

5.1. Lift Force Measurement Test

A second order curve was first used to approximate the relationship between the measured fuel assembly lift force and measured pump flow rate. Coefficients were determined for a best fit relation between lift force and flow rate. The approximated relationships between pump flow rate and measured lift force, for each temperature condition, are plotted in Figure 5.1-1.

Next, two relations regarding the rod bundle average flow velocity were determined. The relationship between the rod bundle average flow velocity and lift force can be seen in Figure 5.1-2, for each temperature condition. The relationship between the rod bundle average flow velocity, v, and the pump flow rate, Q, are also obtained.

Finally, relations between flow in the rod bundle and flow from the pumps were obtained. The relationship between the rod bundle flow velocity and pump flow rate, for each temperature condition, is shown in Figure 5.1-3.

5.2. AFD Tests

Damping ratio and frequency vibration characteristics under pluck test conditions were obtained for still water and axial flow ([   ]) test conditions. The test parameters for all AFD tests are summarized in Table 3.2-1. The "Damping ratio (-)" and "Frequency (Hz)" are obtained using the initial displacement and first response method described earlier.

Summaries of the AFD test results are shown in the following figures. Figures 5.2-1 shows the still water damping ratio and frequency results versus the average amplitude. Figures 5.2-2 through 5.2-4 show the damping ratio and frequency results for the AFD tests with axial flow at different temperatures. In each figure, results are shown for several flow conditions (Still Water (0%TDF), [   ]).

5.3. Evaluation

The AFD test results show that:

Figure 5.1-1   Pump Flow Rate versus Fuel Assembly Lift Force

Figure 5.1-2   Estimated Lift Force versus Rod Bundle Average Flow Velocity, estimated using determined Pressure Loss Coefficient
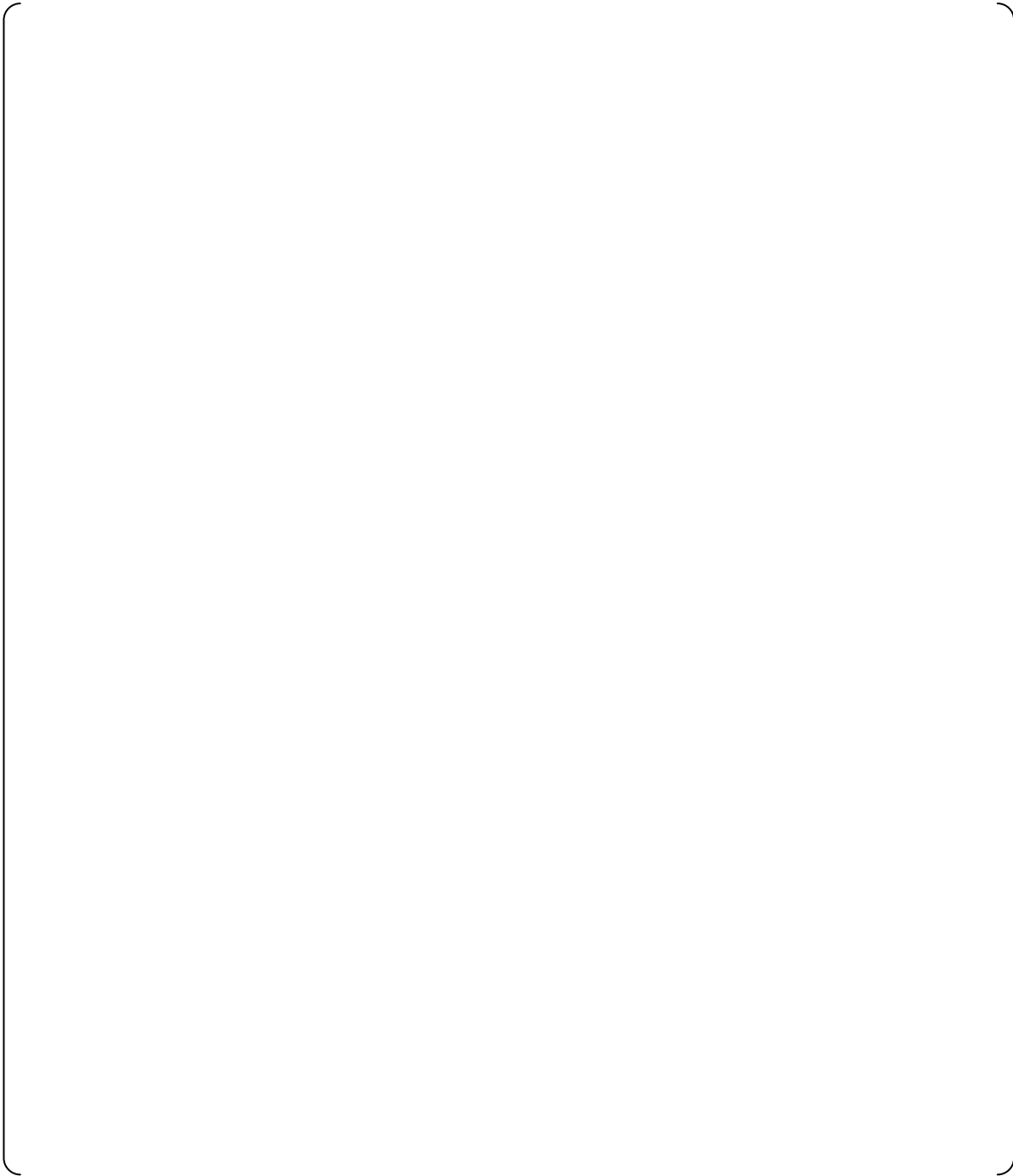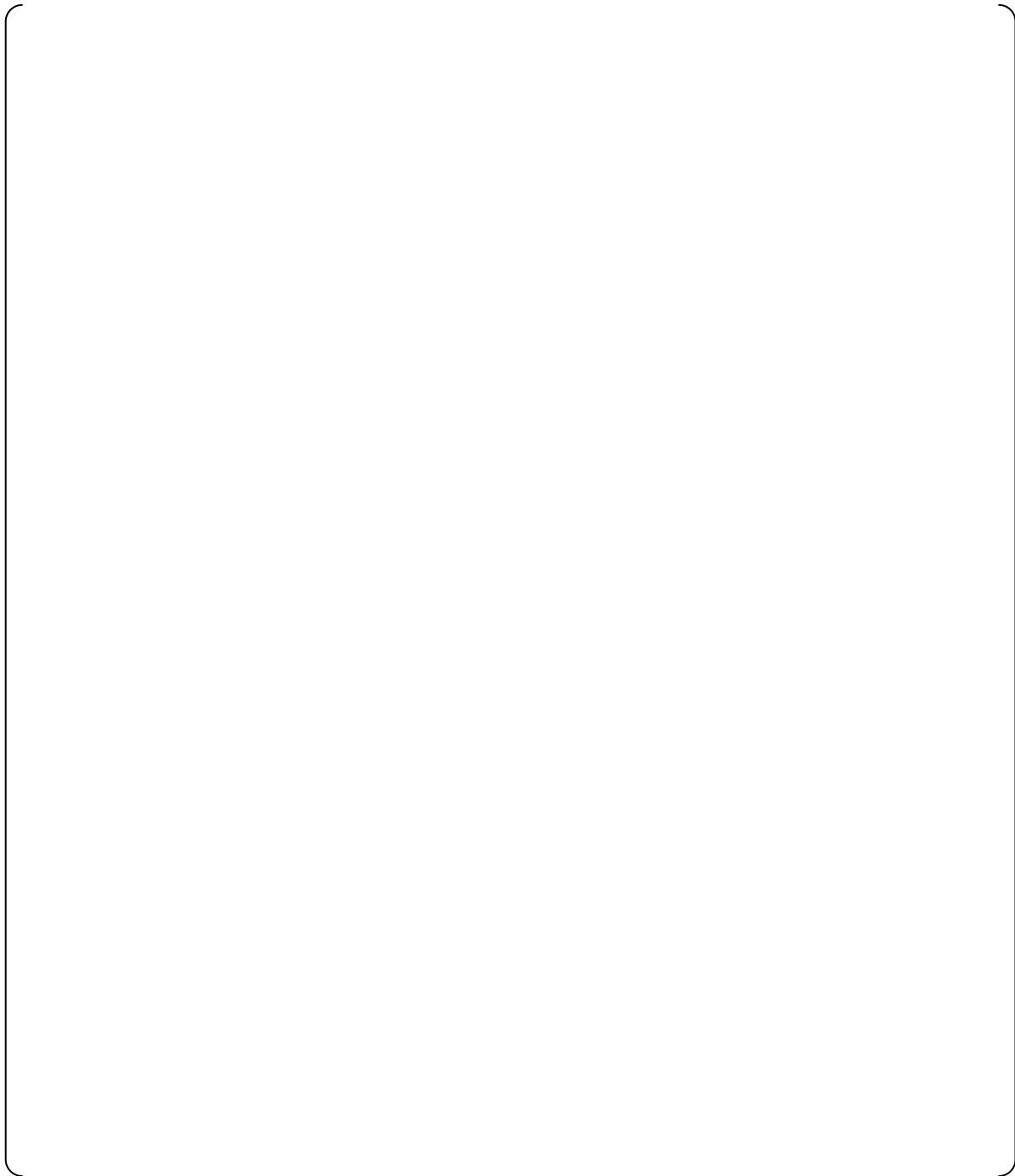
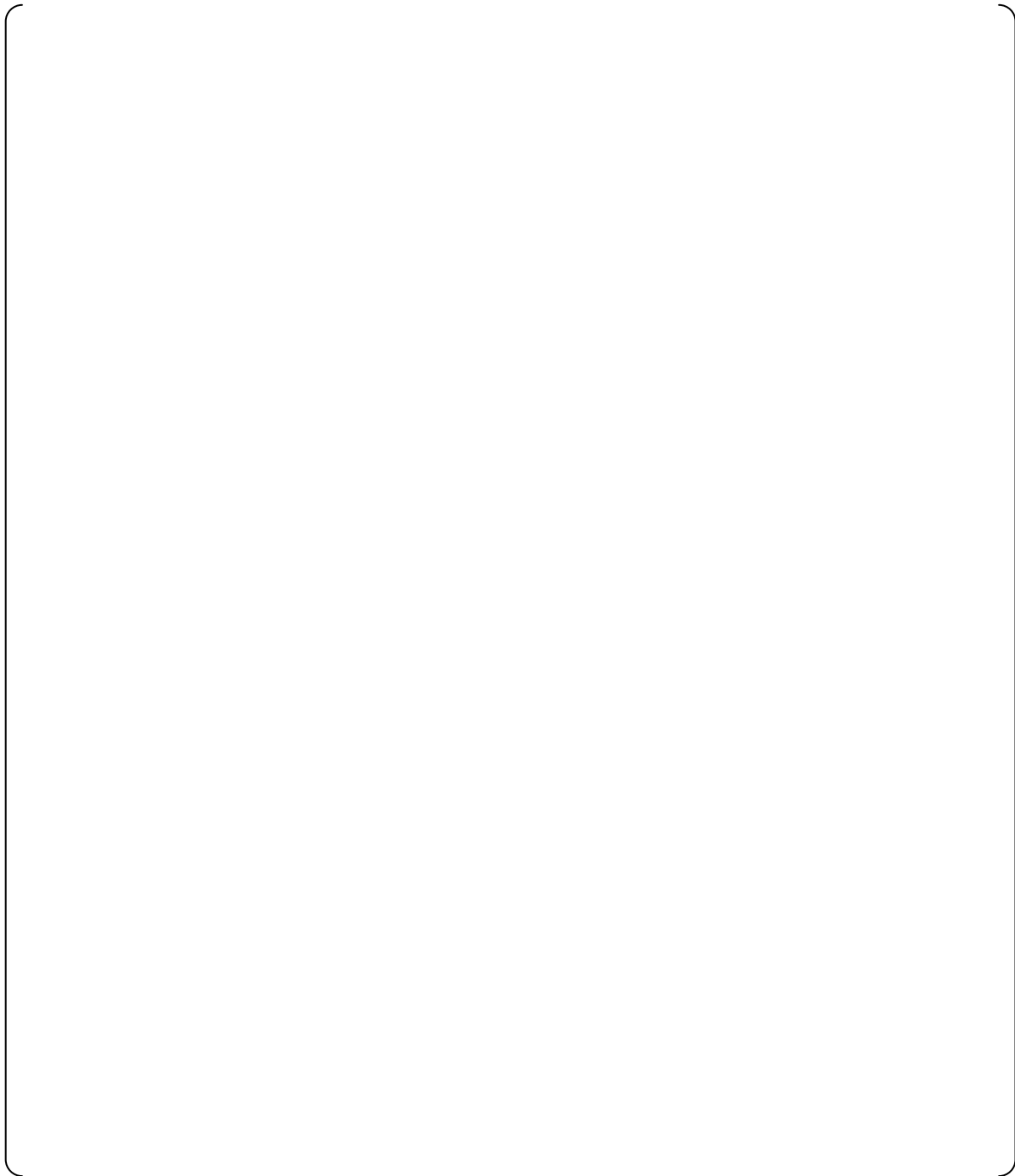**Figure 5.1-3   Summary of Bundle Flow Velocity versus Pump Flow Rate**

**Figure 5.2-1   Damping Ratio and Frequency versus Average Amplitude
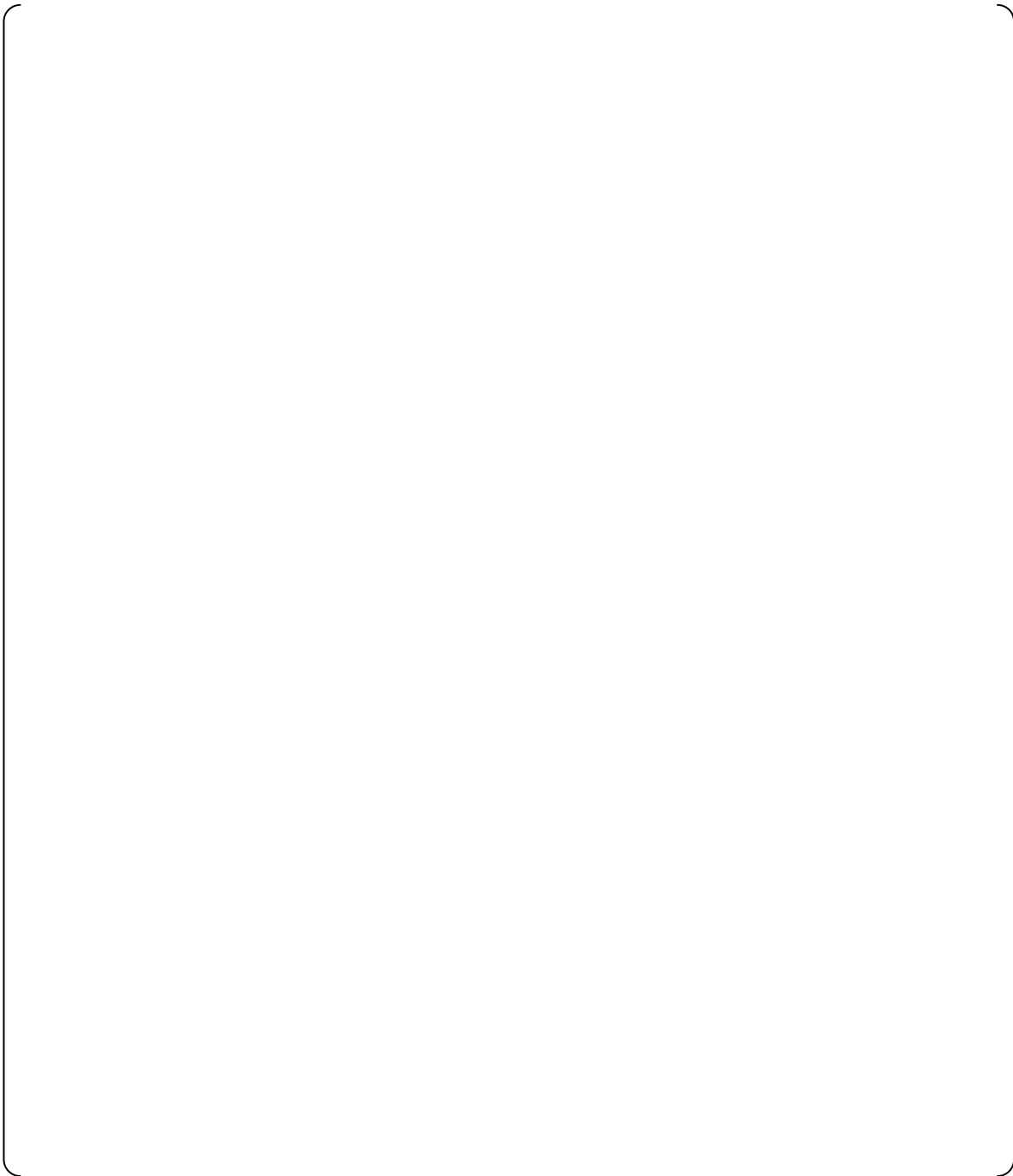(Still Water)**

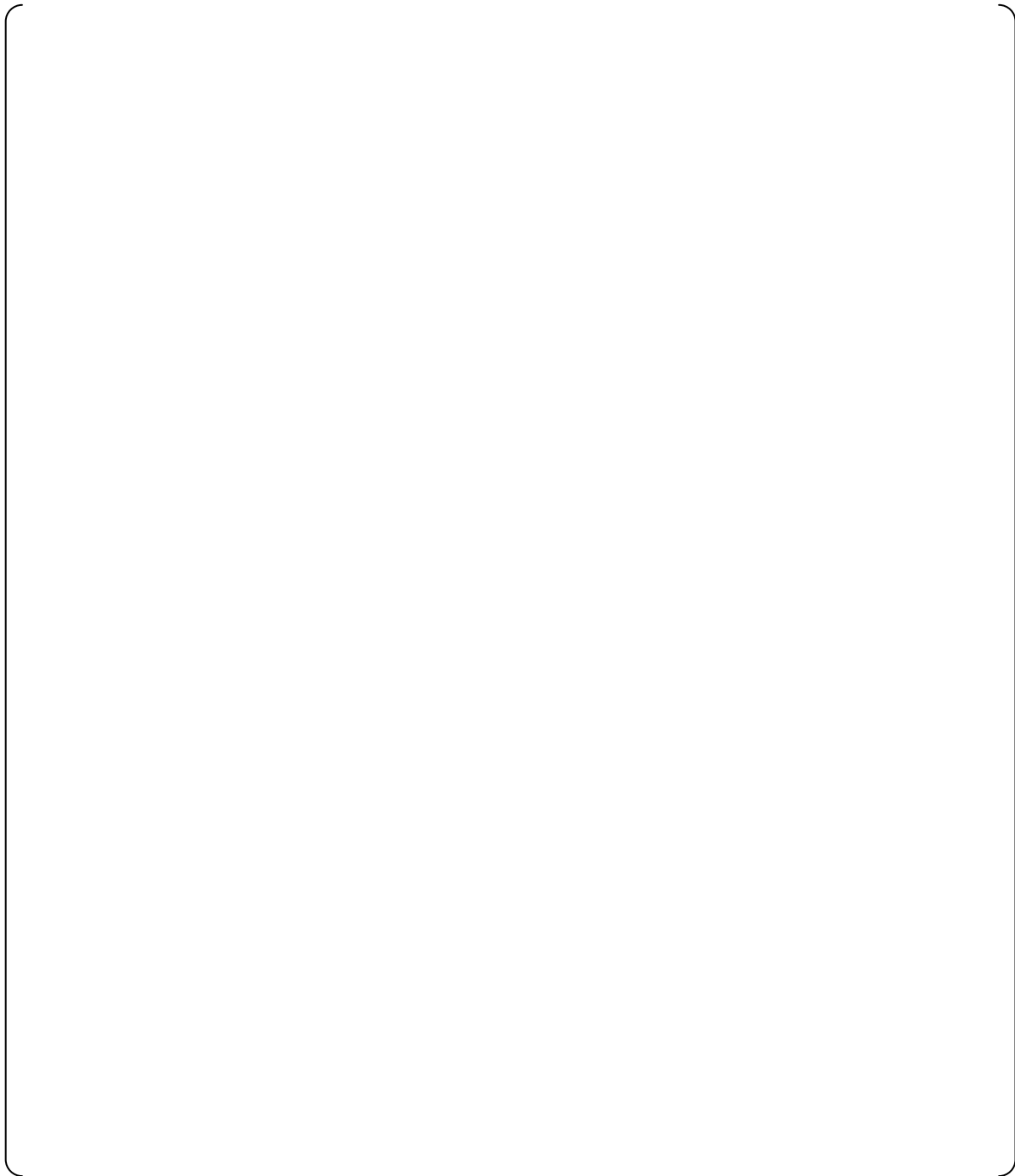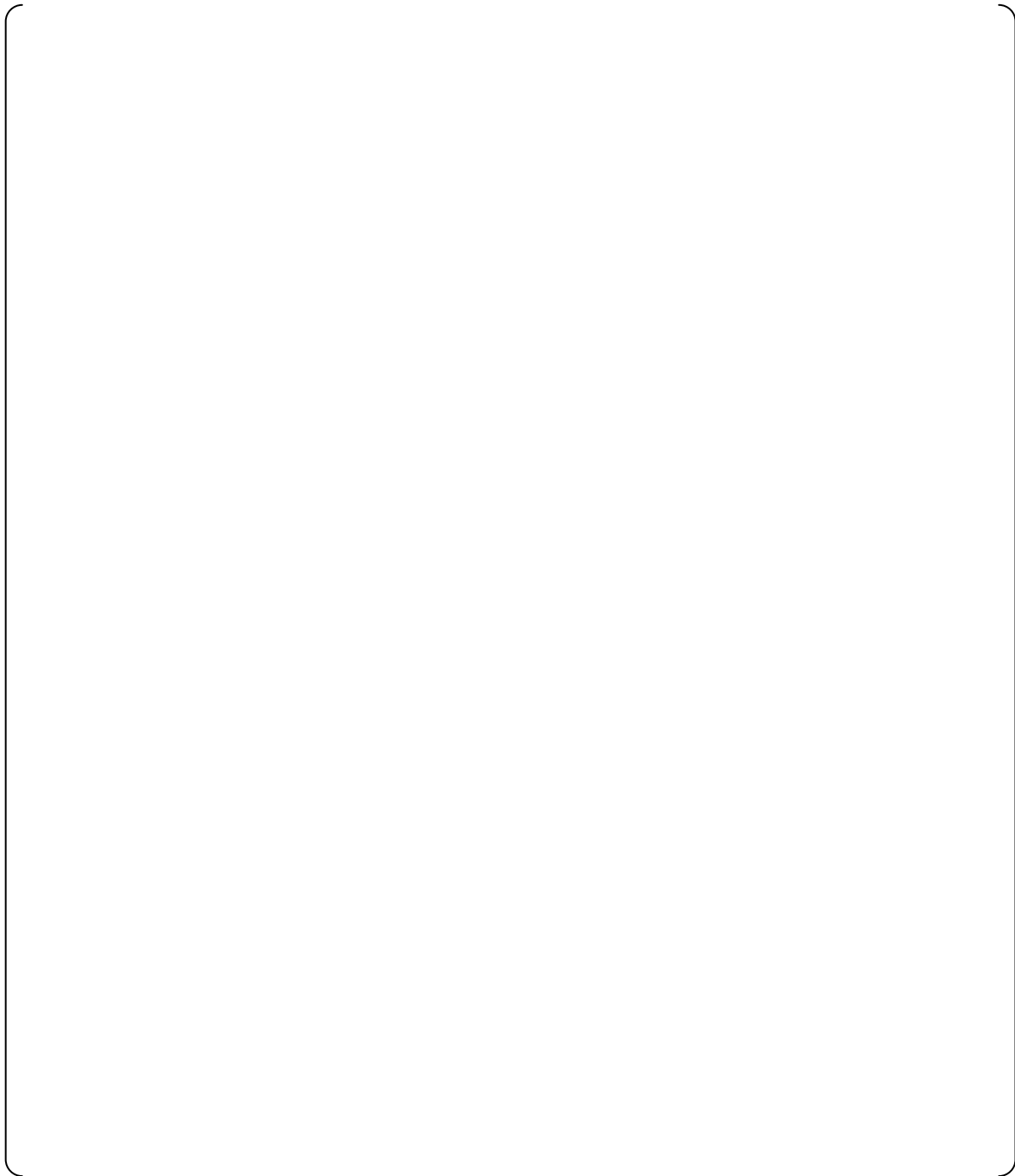**Figure 5.2-2 (1/4)   Damping Ratio and Frequency versus Average Amplitude**
[   ]

Figure 5.2-2 (2/4)   Damping Ratio and Frequency versus Average Amplitude
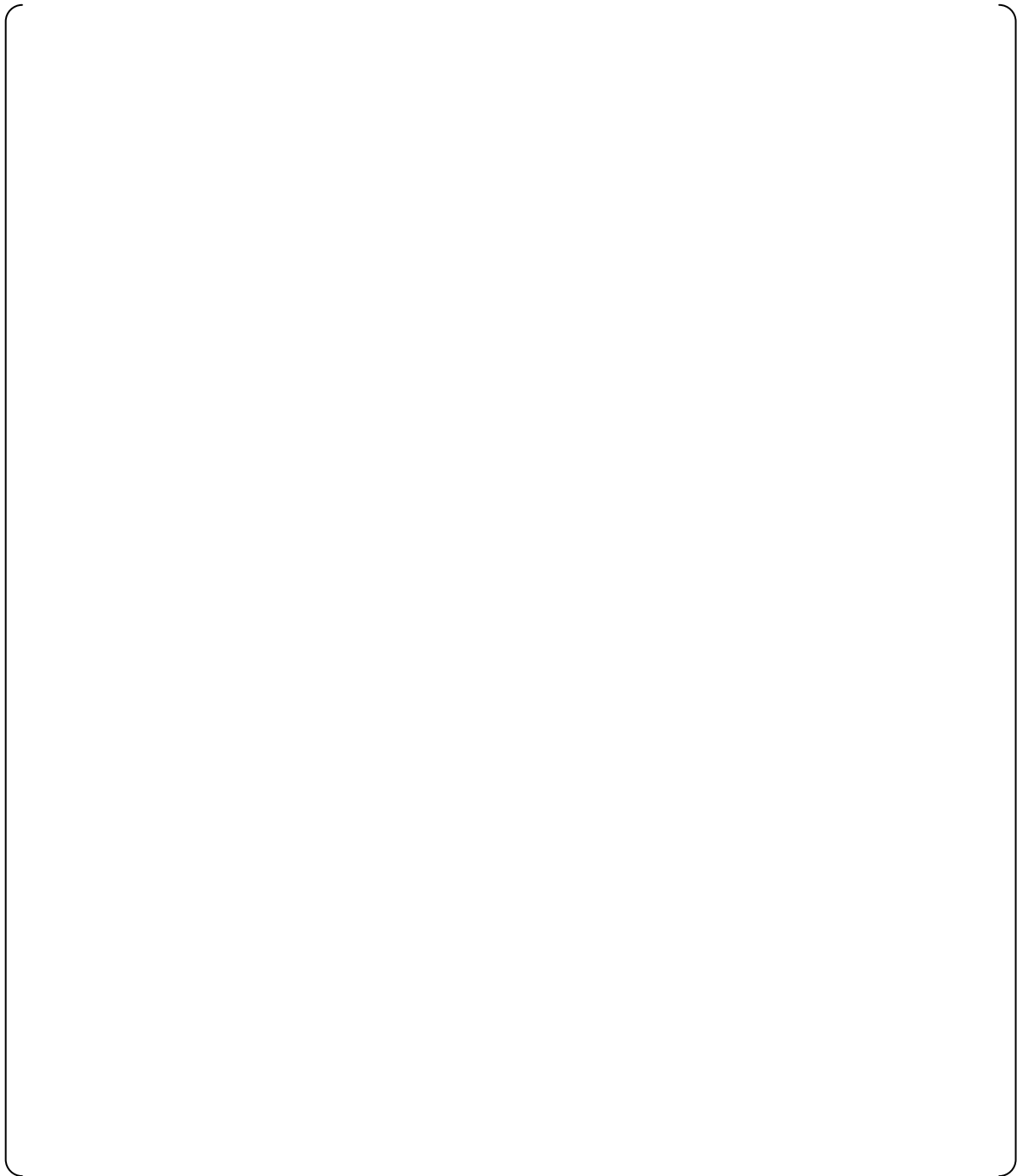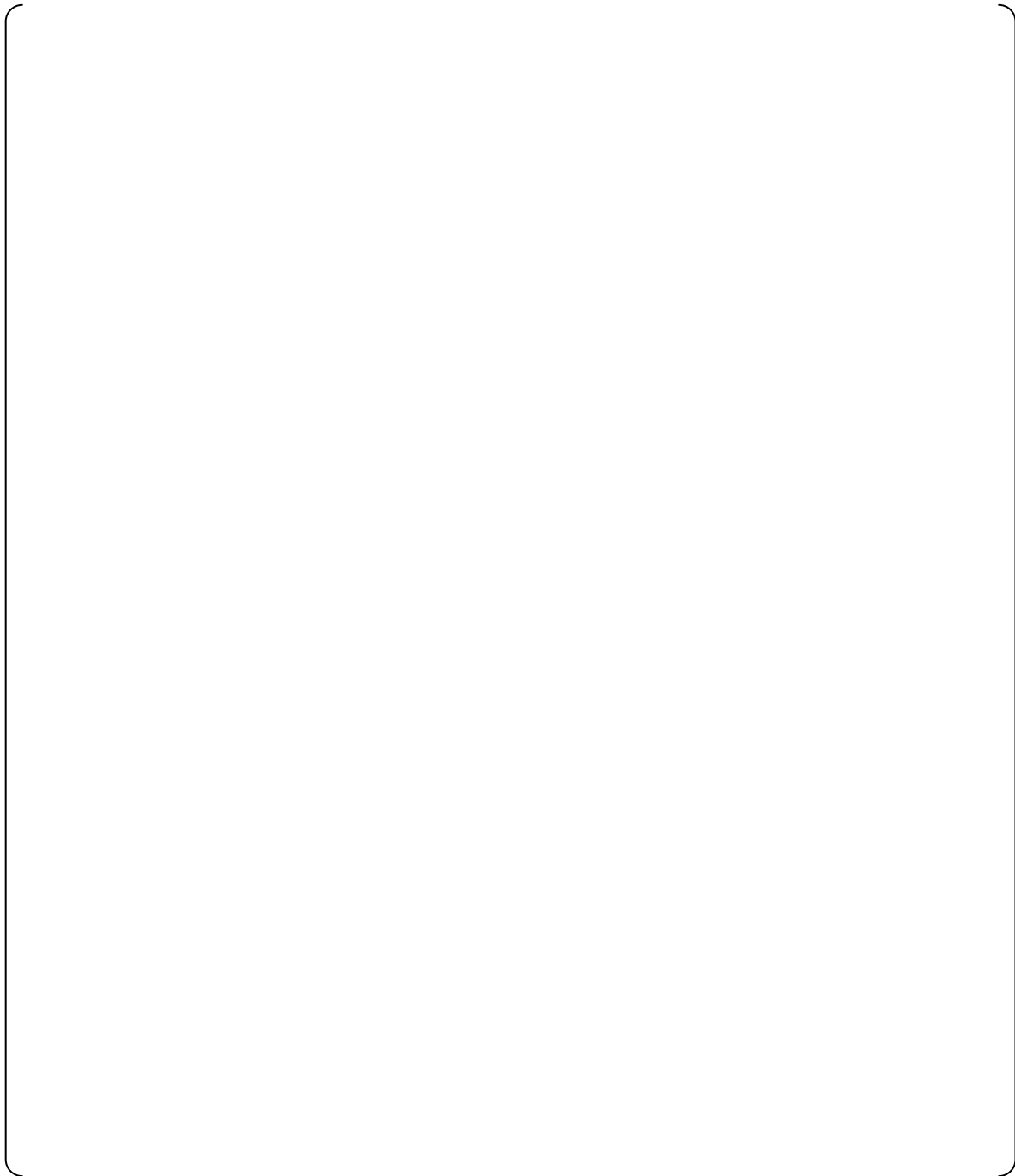[   ]

Figure 5.2-2 (3/4)   Damping Ratio and Frequency versus Average Amplitude
[   ]

Figure 5.2-2 (4/4)   Damping Ratio and Frequency versus Average Amplitude
[   ]

Figure 5.2-3 (1/4)   Damping Ratio and Frequency versus Average Amplitude
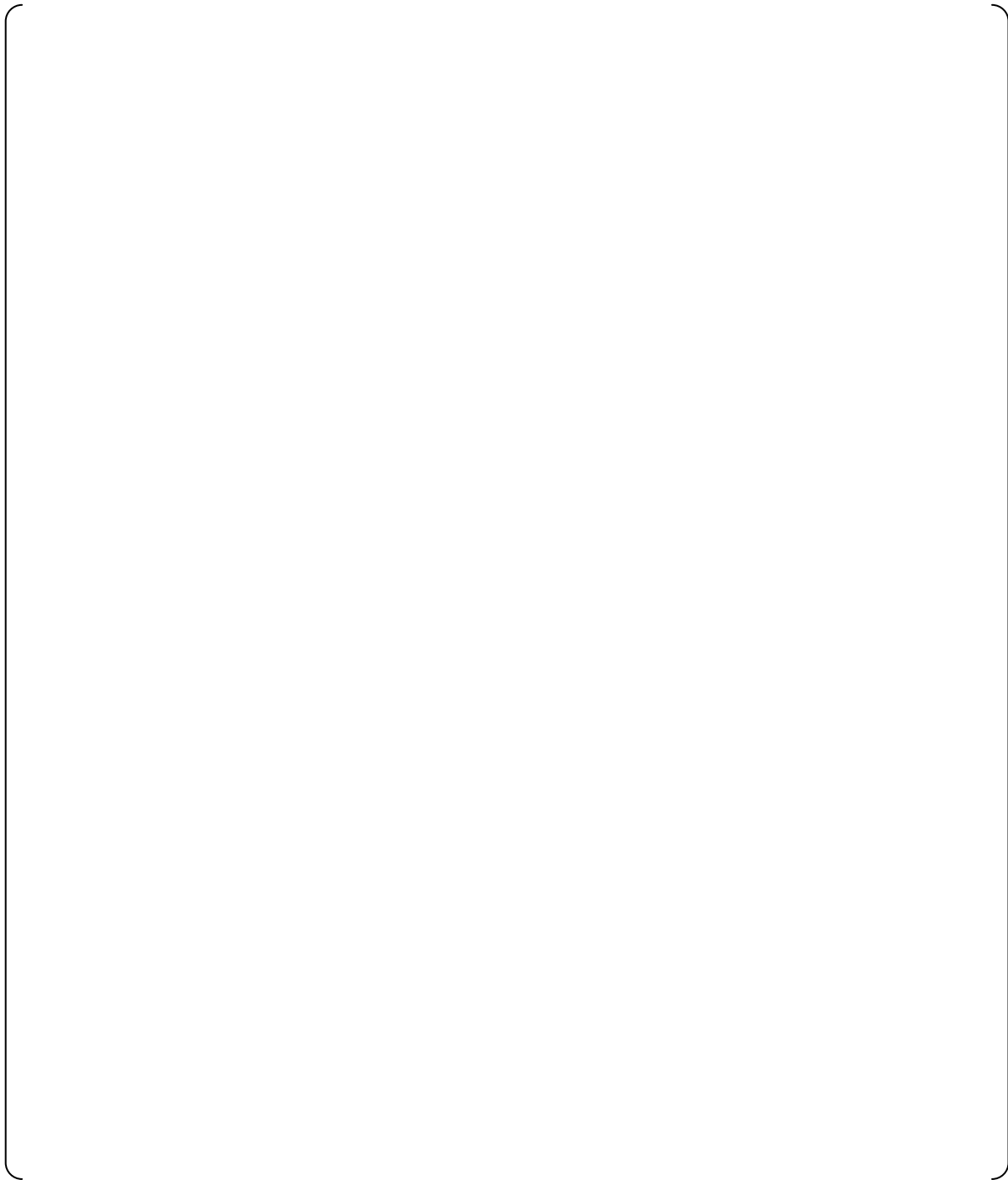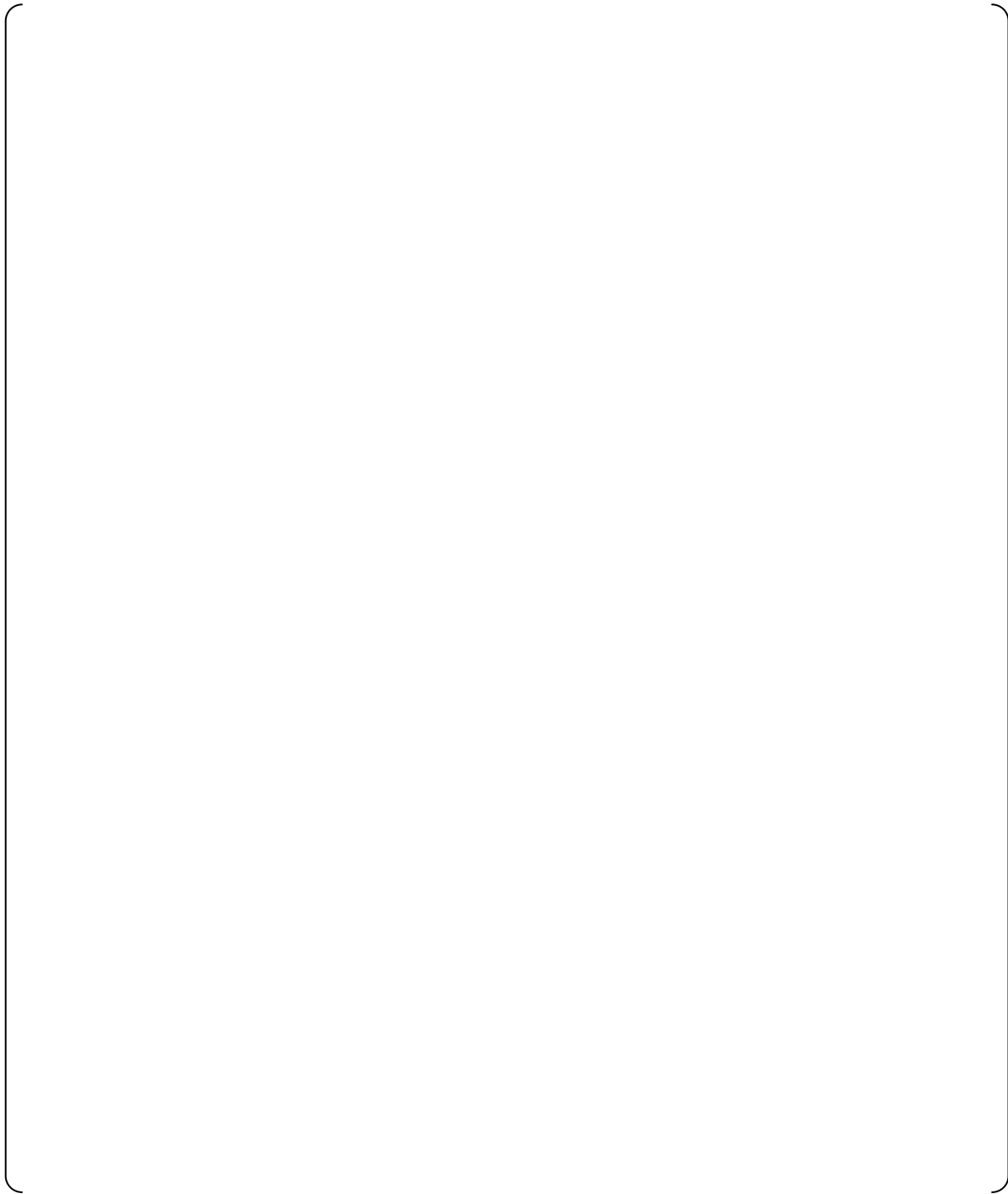[   ]

Figure 5.2-3 (2/4)   Damping Ratio and Frequency versus Average Amplitude
[   ]

Figure 5.2-3 (3/4)   Damping Ratio and Frequency versus Average Amplitude
[   ]

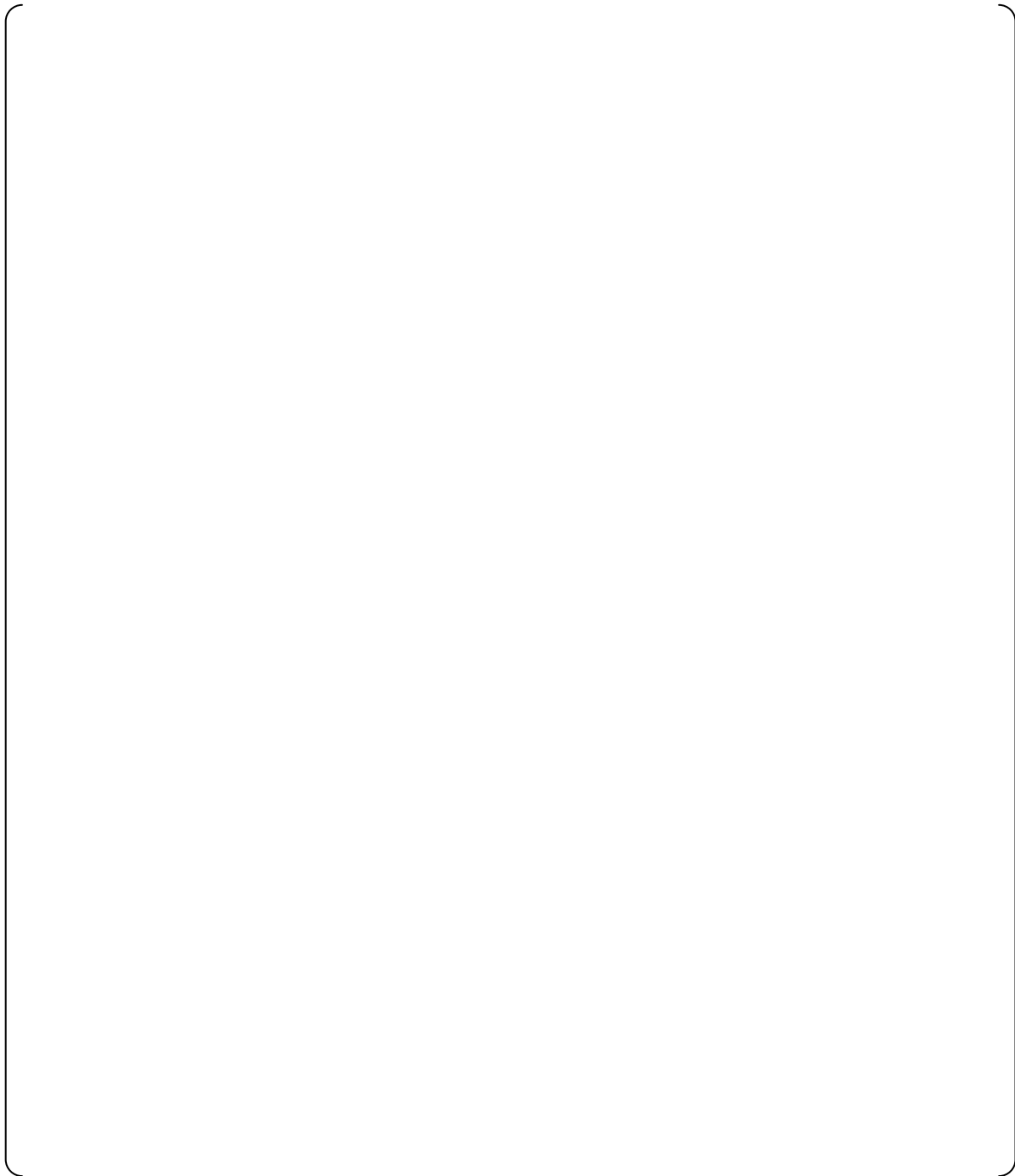**Figure 5.2-3 (4/4)   Damping Ratio and Frequency versus Average Amplitude**

[   ]
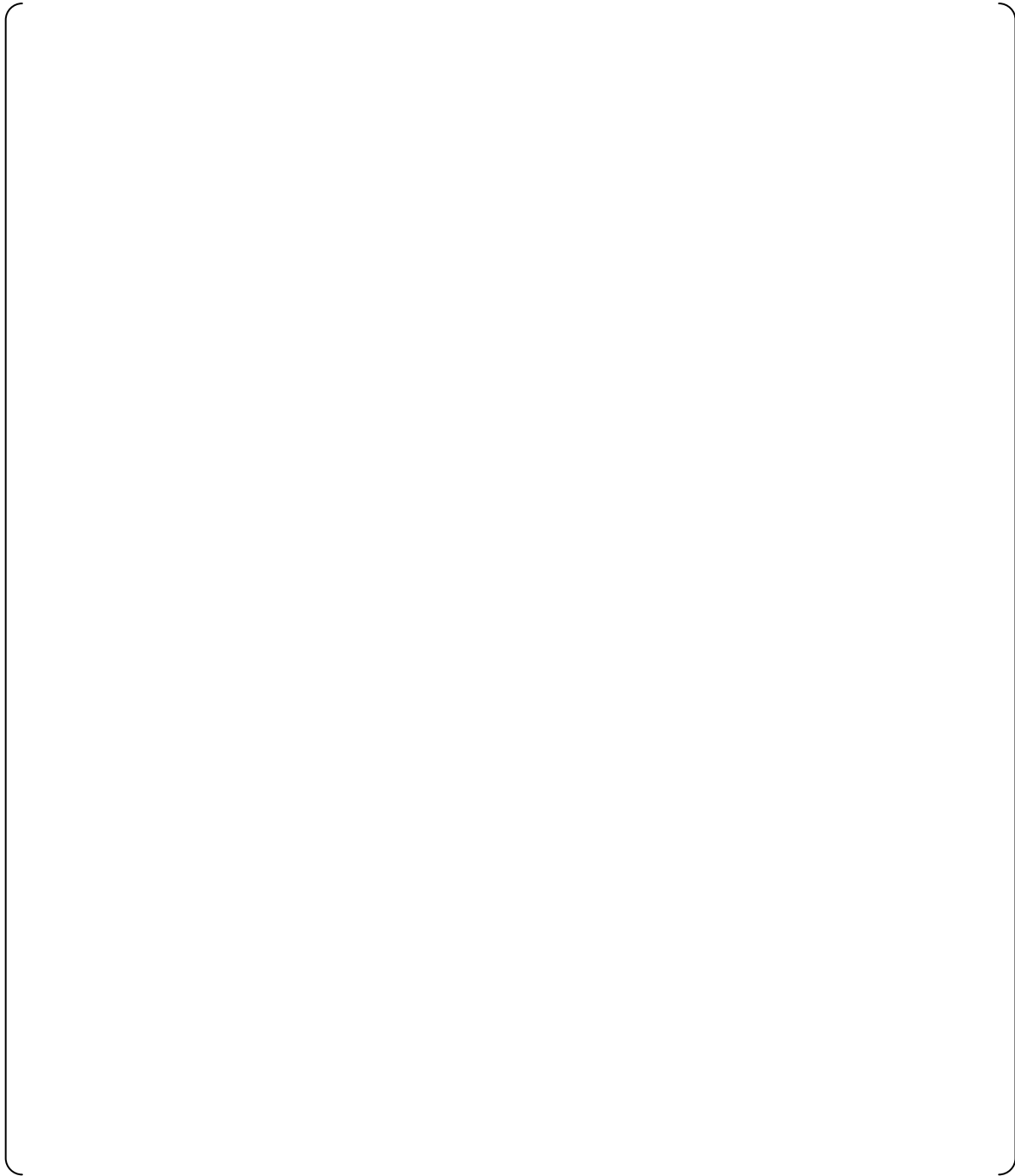
Figure 5.2-4 (1/4)   Damping Ratio and Frequency versus Average Amplitude
[   ]
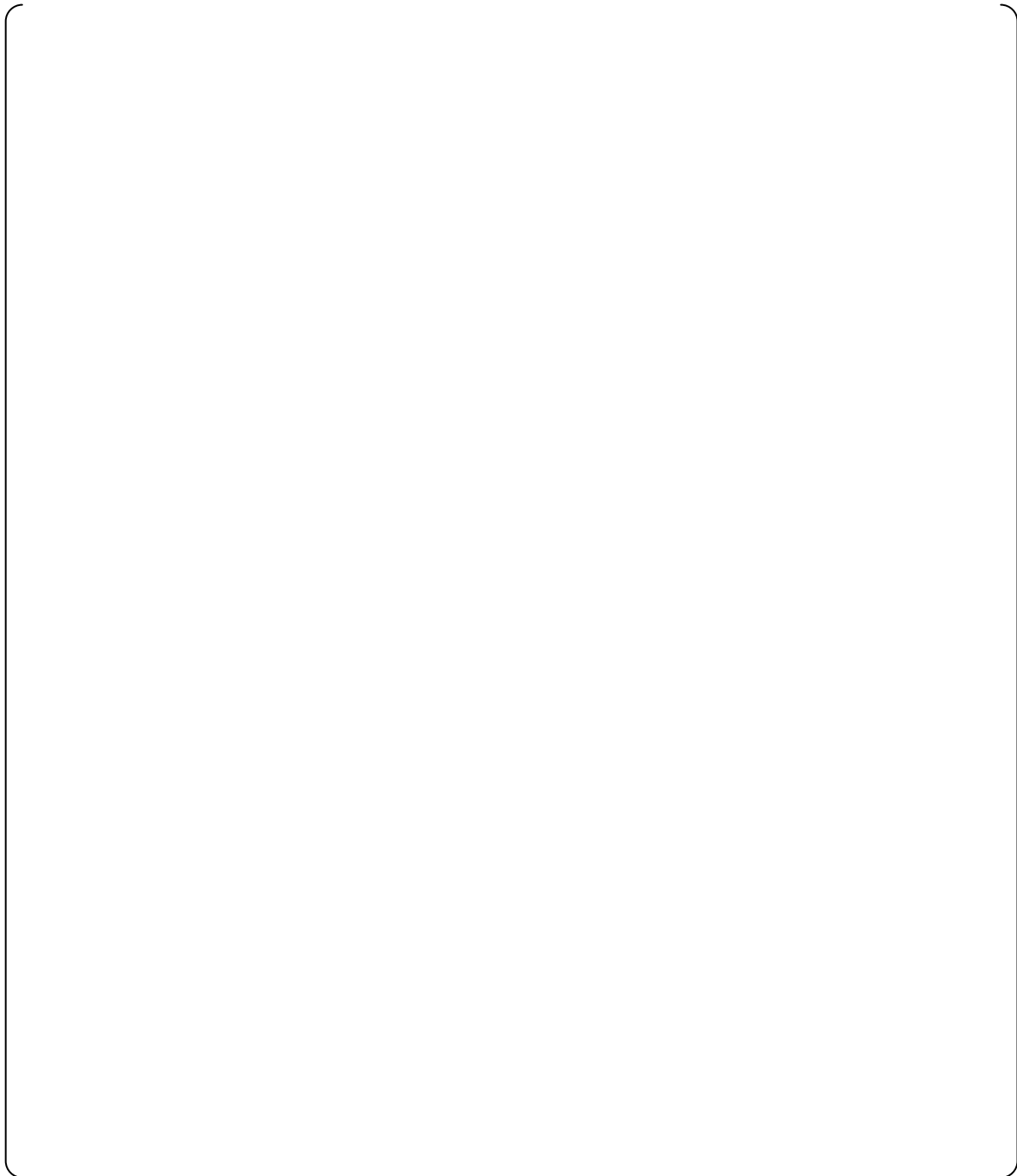
Figure 5.2-4 (2/4)   Damping Ratio and Frequency versus Average Amplitude
[   ]

Figure 5.2-4 (3/4)   Damping Ratio and Frequency versus Average Amplitude
[   ]
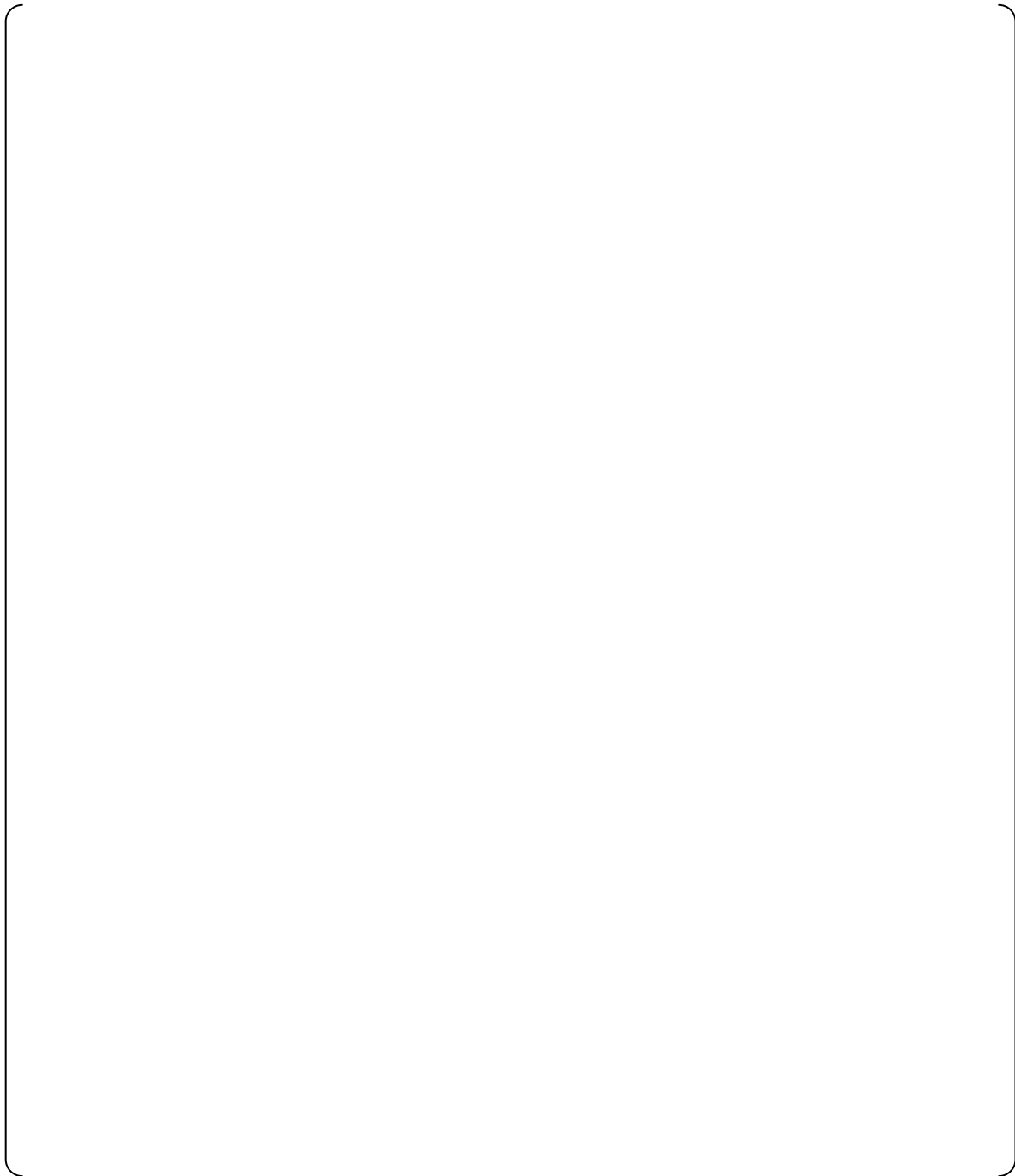
Figure 5.2-4 (4/4)   Damping Ratio and Frequency versus Average Amplitude
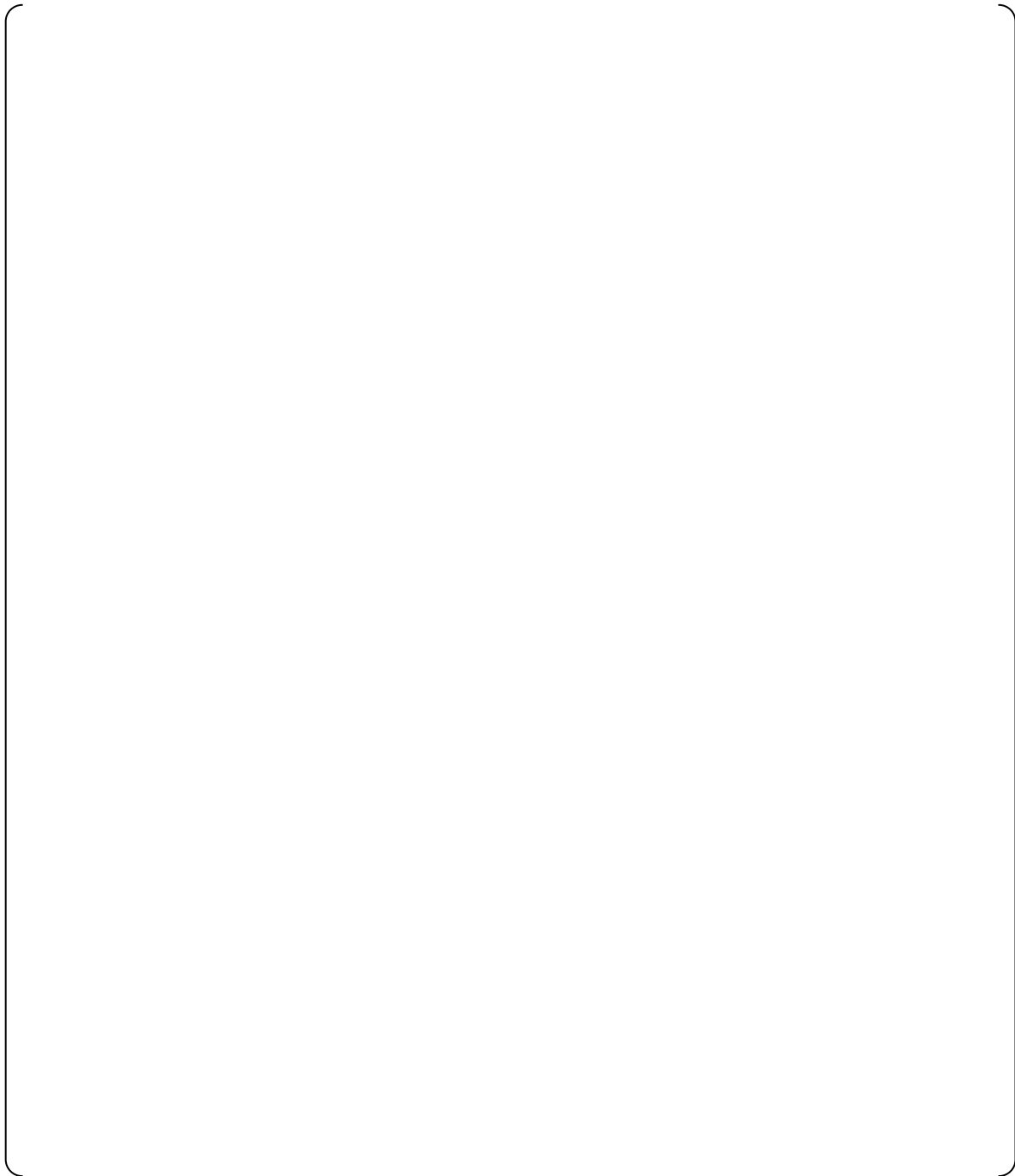[   ]

**Figure 5.3-1 (1/4)   Damping Ratio and Frequency versus Average Amplitude
at Each Temperature Conditions (Still Water)**

**Figure 5.3-1 (2/4)   Damping Ratio and Frequency versus Average Amplitude
at Each Temperature Conditions** [   ]

**Figure 5.3-1 (3/4)   Damping Ratio and Frequency versus Average Amplitude
at Each Temperature Conditions** [   ]

**Figure 5.3-1 (4/4)   Damping Ratio and Frequency versus Average Amplitude
at Each Temperature Conditions** [   ]

6.0 CONCLUSIONS

The axial flow damping tests were performed at room temperature in the still water testing, at three different temperature conditions with axial flow. Various flow rates, dependent on TDF, were tested at each temperature. Multiple fuel assembly initial displacements were applied at each condition. Based on the test, the amplitude dependent damping ratio and frequency values were obtained.

These results will be used to determine input to the US-APWR fuel seismic response analysis to account for the AFD effect (Reference 1), and the results will be shown in the next revision of MUAP-08007 "Evaluation Results of US-APWR Fuel System Structural Response to Seismic and LOCA loads" (Reference 2).

7.0 REFERENCES

1. Mitsubishi Heavy Industries, Ltd., "FINDS: Mitsubishi PWR Fuel Assemblies Seismic Analysis Code", MUAP-07034-P Revision 4, June 2013.

2. Mitsubishi Heavy Industries, Ltd., "Evaluation Results of US-APWR Fuel System Structural Response to Seismic and LOCA loads", MUAP-08007-P Revision 2, December 2010.

3. Quality Assurance Requirements for Nuclear Facility Applications, ASME Boiler and Pressure Vessel Code NQA-1 1994.Edition.

4. Mitsubishi Heavy Industries, Ltd., "Hydraulic Test of the Full Scale US-APWR Fuel Assembly", MUAP-11017-P Revision 0, May 2011.

5. A. Hotta at el., "Parametric Study on Parallel Flow Induced Damping of PWR Fuel Assembly", ASME, PVP-Vol. 191, page 89, 1990

6. W. T. Thomson, "Theory of Vibration with Applications", second edition, 1981, Prentice-Hall.